Efficiency degradation of organic solar cells with solution processed ZnO nanoparticles

P.S. Mbule[1], H.C. Swart[1] and O.M. Ntwaeaborwa[1]
[1]Department of Physics, University of the Free State, Bloemfontein, ZA9300, South Africa

E-mail: mbuleps@gmail.com

Abstract: In this study we investigated the performance of organic solar cells (OSCs) with ZnO nanoparticles used as electron extraction layer (EEL). The device was fabricated by spin-coating poly(3,4-ethylenedioxythiophene) poly(styrenesulfonate) (PEDOT:PSS) polymer on a glass substrates pre-coated with a layer of transparent indium-tin-oxide (ITO) followed consecutively by layers of a blend of poly(3-hexylthiopene) (P3HT) and [6,6] –phenyl C_{61}-butyric acid methyl ester (PCBM), ZnO nanoparticles and evaporation of aluminium metal as cathode electrode. The power conversion efficiency (PCE) of 2.37 % was recorded from the OSC device incorporating a concentration of 0.5 mg/ml ZnO nanoparticles EEL and the PCE of 0.20 % was recorded from the same device after 10 days of storage in ambient laboratory conditions. The mechanisms of degradation of the OSC devices are discussed.

1. Introduction

Organic photovoltaic devices have drawn a lot of attention as means for the renewable energy conversion due to the remarkable combination of prospective low cost of manufacturing and rapid improvement of performance promising to approach the traditional silicon solar cells [1]. By introducing metal oxides in organic photovoltaics, the organic solar cells show great potential in terms of device performance with high exciton dissociation, the favourable charge transport ability and the air stability [2]. One of the key solar cell parameters affecting the cell power conversion efficiency (PCE) is the series resistance or internal resistance, R_s. The series resistance represents the total resistance of the cell and is a composite of (i) the active and interfacial layer resistances, (ii) electrode resistances and (iii) the various contacts and interconnect resistances [3]. Normal geometry of bulk heterojunction (BHJ) organic solar cells can suffer degradation of the top electrode, which is normally made of a low-work function metal (Al) that is reactive and oxidize easily in air. The exposure of Al cathode can cause oxidation and degradation of the active layer due to the diffusion of oxygen and moisture through pinholes and grain boundaries [4].

---

[1] Mbule P.S, Email: mbuleps@gmail.com

2. Experimental

2.1. ZnO nanoparticles synthesis

ZnO nanoparticles were synthesized by hydroxylation of zinc acetate dihydrate (ZnAc.2H$_2$O) by tetramethylammonium hydroxide (TMAH). In a typical preparation, TMAH dissolved in 30 ml of ethanol was added dropwise to 0.1M zinc acetate dihydrate dissolved in 30 ml of dimethylsulfoxide (DMSO). The nanoparticles were precipitated by adding ethyl acetate and then washed at least 3 times with heptane. Then nanoparticles were dried at 110 ^{o}C in an oven or re-dispersed in methanol. Figure 1 shows the schematic diagram of the ZnO synthesis.
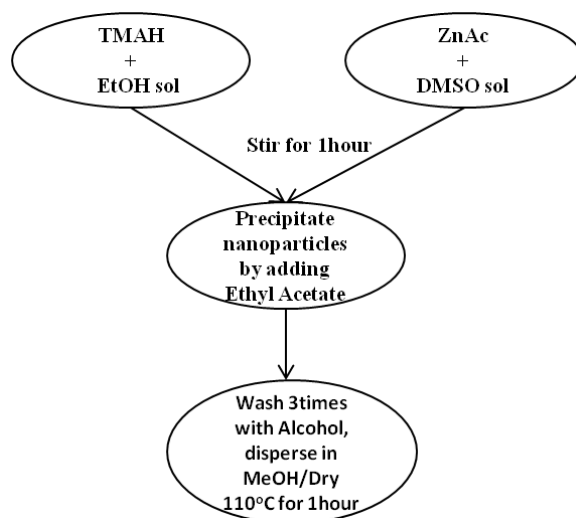

Figure 1: Schematic diagram of ZnO nanoparticles synthesis

2.2. Device Fabricaion

The organic solar cell device consisting of successive layers PEDOT:PSS (hole extraction layer), P3HT:PCBM (photo-active layer), ZnO nanoparticles (electron extraction layer) and Al cathode spin-coated on a glass substrate pre-coated with a layer of transparent indium-tin-oxide or ITO (anode) was fabricated. The glass substrate was first cleaned ultrasonically using isopropanol followed by drying at ~80 ^{o}C for 20 min and was finally treated in an ultraviolet ozone generator for 20 min. A thin layer of poly(3,4-PEDOT:PSS (CLEVIOS™ AI 4083) was spin-coated on the cleaned ITO pre-coated glass substrate at the speed of 4000 rpm for 35 s followed by drying in an oven/hot plate at 110 ^{o}C for 10 min. The active layer of P3HT:PCBM blend with a weight ratio of 1:0.6, dissolved in chlorobenzene, was spin-coated at the speed of 1000 rpm for 15 s. This was followed by the deposition of the layer of methanol solution of 0.5 mg/ml ZnO nanoparticles at 4000 rpm for 35 s. The top Al metal electrode (~100 nm) was thermally evaporated at ~ 1 x 10^{-6} Torr pressure through a shadow mask and the device area was 0.12 cm^2.

ZnO nanoparticles film structure was analyzed by X-ray diffractometer (XRD). The morphology of nanoparticles was determined by Field emission scanning electron microscopy (FE-SEM). The current density-voltage (J-V) curves of the device was measured in air using a Keithley 2400 source meter and an Oriel xenon lamp (150 W) coupled with an AM1.5 filter to simulate sunlight. The light intensity was calibrated with a silicon reference cell with a KG2 filter following standard solar cell testing procedures. All J-V measurements were conducted at the light intensity of 100 mW/cm^2. And finally SIMS depth profiling was performed by iontof TOF-SIMS[5] using two depth profiling ion beams operating in dual beam mode (Cs$^+$ ions for sputtering and Bi^{3++} for analyzing) to analyse the interface of different layers in the device.

3. Results and discussion

XRD patterns of ZnO nanoparticles are shown in figure 2. The diffraction peaks at scattering angles of 31.8 °, 34.4 °, 36.3 °, 47.5 °, 56.5 °, 62.7 °, 66.3 °, 67.9 ° and 69.0 ° correspond to the reflection from (100), (002), (101), (102), (110), (103), (200), (112) and (210) crystal planes, respectively, and they match well with the standard JCPDS data, card number 80-0075. Furthermore, the XRD data indicate that ZnO nanostructures exhibit the hexagonal wurtzite structure and the Debye-Scherrer equation [5] was used to estimate the crystallite size which was found to be ~ 5 ± 0.2 nm. FE-SEM images of spherical ZnO nanoparticles were observed and nanoparticles are evenly distributed on the surface. This is shown in figure 3.
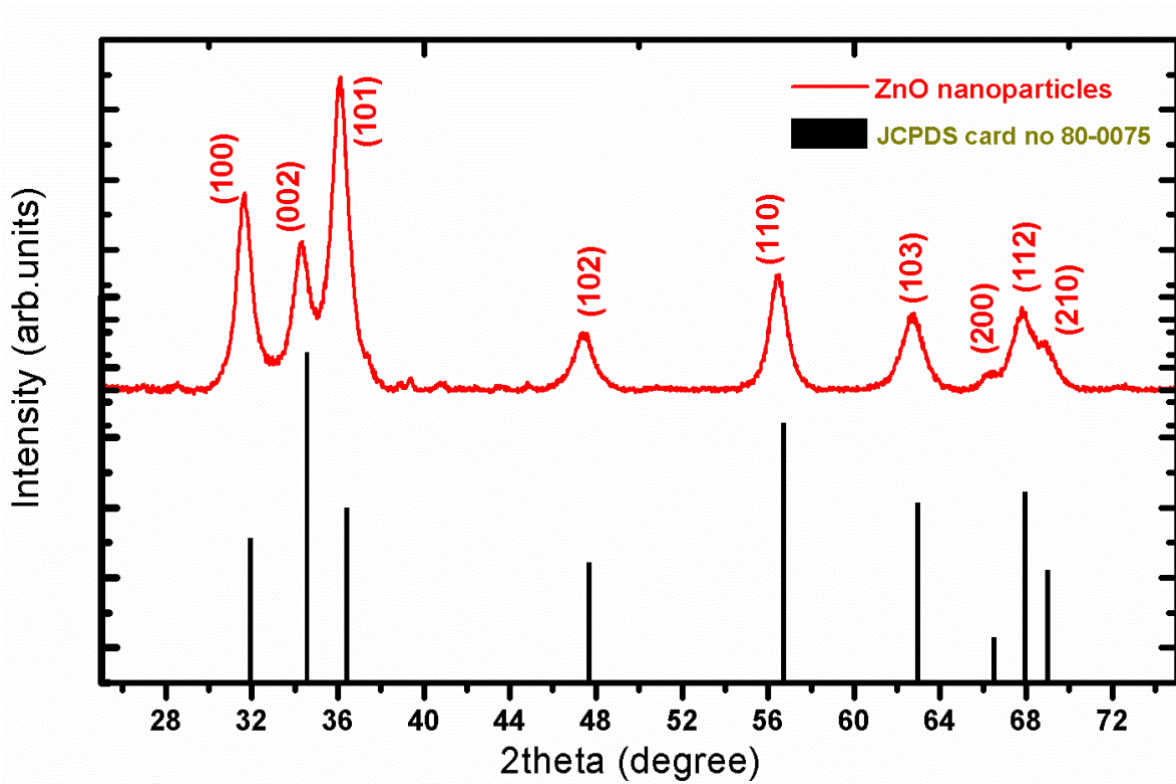

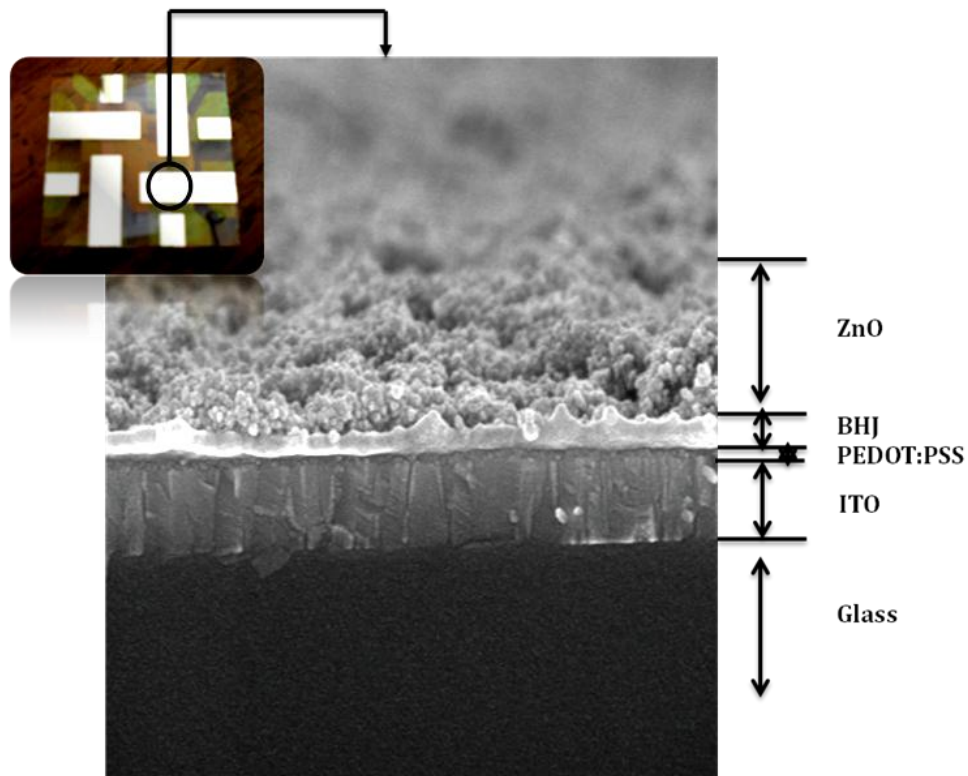**Figure 2:** XRD patttern of ZnO nanoparticles.

Figure 3: An image of a complete conventional organic solar cell and the FE-SEM cross-sectional view showing the different components of the device.

The Photovoltaic (PV) response curves of the device are illustrated in figure 4 with the summary of the PV characteristics presented in table 1. The initial device characteristics under solar irradiation in air yielded a power conversion efficiency of 2.37 %. The device significantly degraded after 10 days of storage with encapsulation in ambient laboratory conditions resulting in an efficiency of 0.20 %. The reduction of efficiency results primarily from a decrease in the short circuit current density and the degradation of active layer materials. There are different factors that can cause degradation of the OSC device and these factors can be classified as physical and/ or chemical. Generally, large serial resistances due to degradation of the bulk of a material or the quality of the metal electrode reduce the performance of the device. As observed in figure 4, after 10 days of storage the device suffers large series resistance, significantly increasing from 217 to 13 552 Ωcm^2. This is due to the deterioration of charge transport in the layers. The reduced fill factor (FF) from 49.50% to 37.18 % could be due to the reduced interfacial charge transfer efficiency between different layers [6]. Additionally, the degradation can be localized in the electrode layer itself or at the electrode/ZnO layer/active layer interfaces. In this last case, the degradation mechanism generally leads to a decrease of the interface quality between the active layer/ZnO layer and the electrode, therefore leading to a reduction of the charge transfer and extraction. This reduction of electrode/active layer interface can be due to physical loss of contact between the layers due to delamination [7], creation of voids or the formation of electrically insulating patches at the interface due to change of chemical reactions at the surface of the metal electrode [8]. Moreover, Positive secondary ion polarity, SIMS depth profiling of the device is presented in figure 5. Signals arising from different layers of the device components are clearly identified and the diffusion of tin (^{120}Sn) and indium (^{115}In) into the active layer has been recognized as one of the main factors that are detrimental to the life time of organic solar cells [9]. Different causes of device degradation are reported elsewhere [10].

Table 1: Photovoltaic comparison of the device

Device after fabrication				
$J_{sc}(mA/cm^2)$	$V_{oc}(V)$	FF(%)	PCE (%)	$R_s\ (\Omega.cm^2)$
7.18	0.67	49.5	2.37	217
Device after 10 days of storage				
$J_{sc}(mA/cm^2)$	$V_{oc}(V)$	FF(%)	PCE (%)	$R_s\ (\Omega.cm^2)$
0.91	0.59	37.18	0.20	13 552
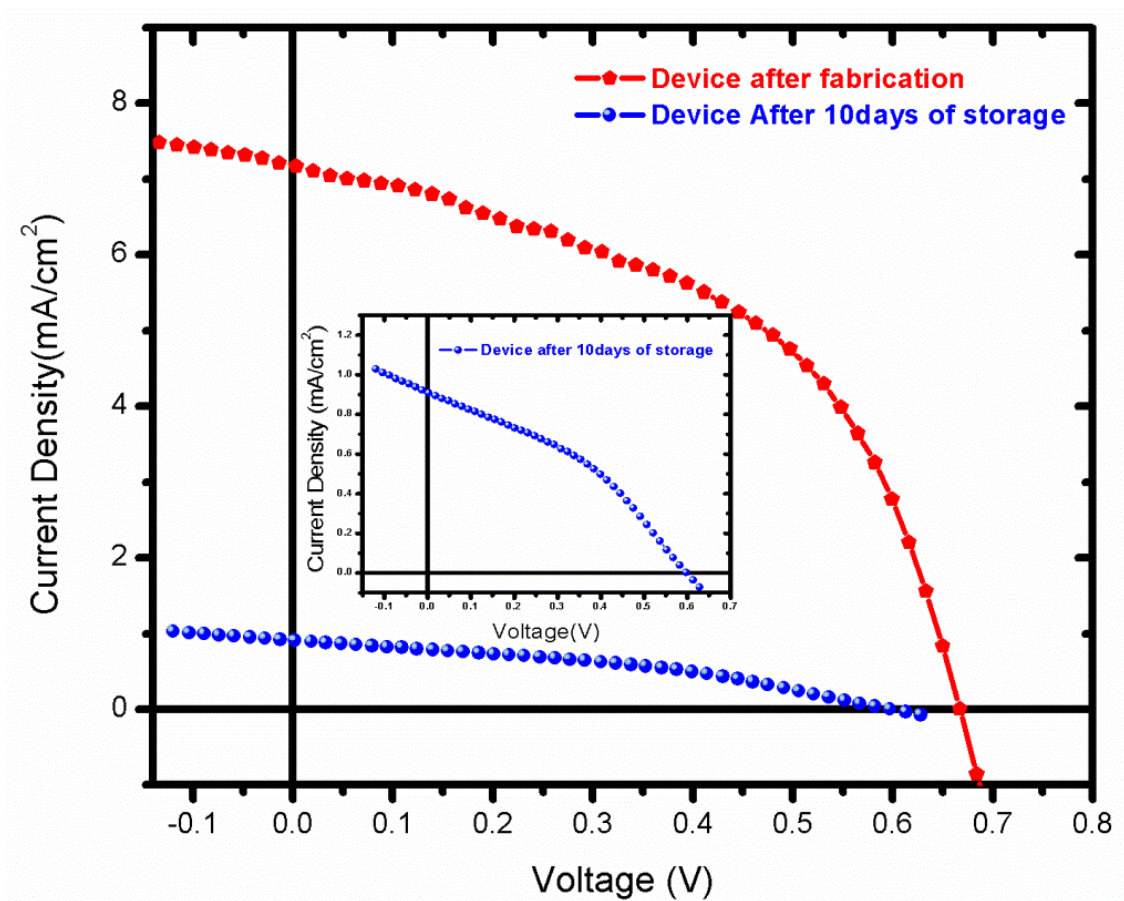
Figure 4: J-V curves of the device after fabrication and 10 days after storage
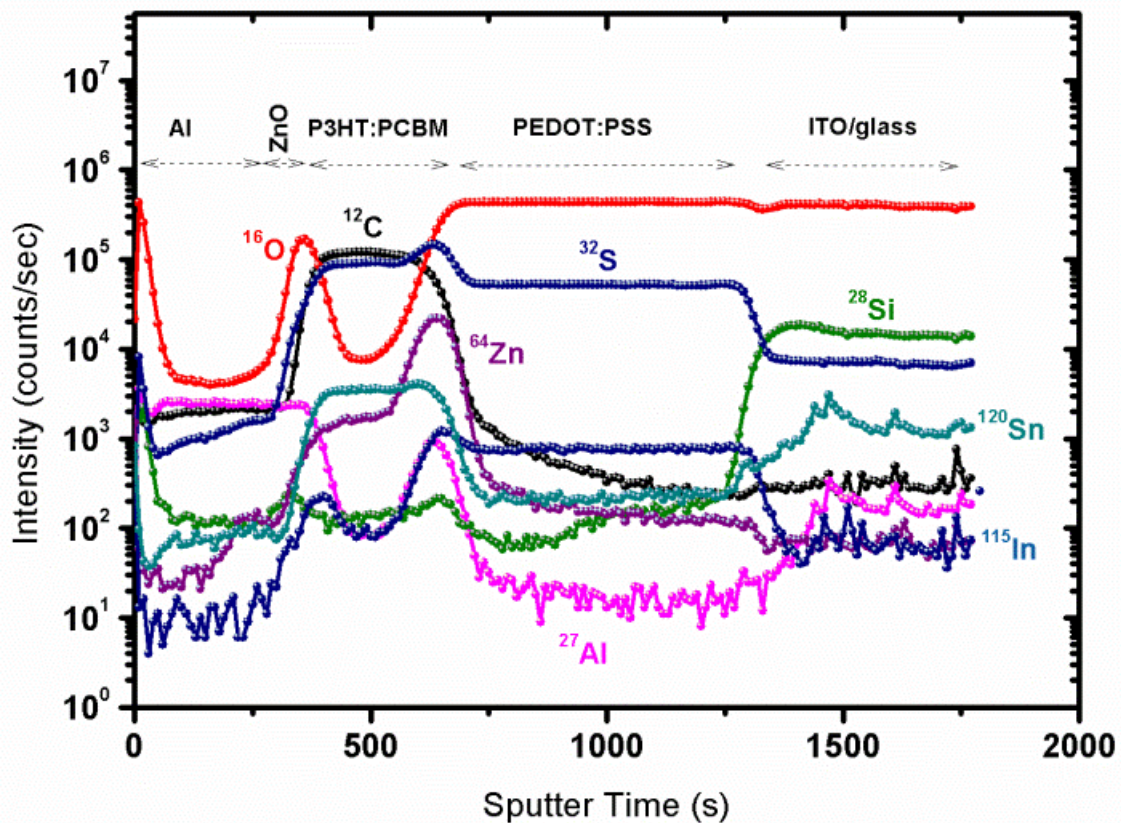
Figure 5: SIMS depth profiles of organic solar cell.

4. Conclusion

In conclusion, deterioration of charge collection in organic solar cell is reported. This is due to chemical degradation or oxidation of the compounds of the photoactive layer caused by atmospheric moisture or oxygen. Furthermore, atoms or molecules resulting from chemical degradation of the electrode can migrate through the other layers of the organic solar cell which may be damaging to the performance of the device. Chemical, physical and interfacial stability in organic devices remain a critical matter since polymeric materials are known to be less durable over a period of time.

References

[1] Ma W, Yang C, Gong X, Lee K and Heeger A.J, 2005 Adv. Funct. Mater. **15** 1617-1622

[2] Sekine N, Chou C.-H, Kwan W.-L and Yang Y, 2009 Org. Electron. **10** 1473-1477

[3] Servaites D.J, Yeganeh S, Marks T.J and Ratner M.A, 2010 Adv. Funct. Mater. **20** 97-104

[4] Wang J.C, Weng W.T, Tsai M.Y, Lee M.K, Horng S.F, Perng T.P, Yu C.C and Meng H.F, 2010 J.Mater. Chem. **20** 862-866

[5] Oh H, Krantz J, Litzov I, Pinna T and Brabec C.J, 2011 Sol. Energy Mater. Sol. Cells **95** 2194-2199

[6] Kawano K, Pacios R, Poplavskyy D, Nelson J, Bradley D and Durrant J.R, 2006 Sol. Energy Mater. Sol. Cells **90** 3520-3530

[7] Reese M.O, White M.S, Rumbles G, Ginley D.S and Shaheen S.E, 2008 Appl. Phys. Lett. **92** 053307/1-053307/3

[8] Paci B, Generosi A, Albertini V.R, Perfetti P, Firon M, Leroy J and Sentein C, 2005 Appl. Phys. Lett. **87** 194110-194110-3

[9] de Jong M.P, van Ijzendoorn L.J and de Voigt M.J.A, 2000 Appl. Phys. Lett. **77** 1212-1214

[10] Grossiord N, Kroon J.M, Andriessen R and Blom P.W.M, 2012 Org. Electron **13** 432-456